

Thermal decomposition of nickel(II), palladium(II), and platinum(II) complexes of *N*-allyl-*N'*-pyrimidin-2ylthiourea

Saud M. A. Katib

Received: 31 May 2010/Accepted: 5 August 2010/Published online: 28 August 2010
© Akadémiai Kiadó, Budapest, Hungary 2010

Abstract Thermal decomposition of Ni(II), Pd(II), and Pt(II) complexes of *N*-pyrimidin-2ylthiourea (AllPmTu) have been studied by TG, DTG, and DTA and by electron impact (EI) mass spectra. The complexes have the molecular formulae as $[Ni(AllPmTu)Cl_2(H_2O)]$, $[Ni(AllPmTu)_2Cl_2(H_2O)_2]$, and $[M(AllPmTu)Cl_2]$, where $M = Pd^{II}$ or Pt^{II} , and $[Pt(AllPmTu)_2]$. The TG curves show that Ni(II) complexes decompose in three stages to yield NiO as a residue, while Pd(II) and Pt(II) decompose in two stages to yield MS residues. The initial mass losses correspond to elimination of allylamine for Pd(II) and Pt(II) complexes but, allylisothiocyanate for both Ni(II) complexes revealing that sulfur atom of thiourea part is involved in coordination to Pd(II) and Pt(II) but does not to Ni(II). Kinetic parameters ($E^\#$, n , $\Delta H^\#$, $\Delta S^\#$, $\Delta G^\#$) of the decomposition stages are determined and correlated with bonding and structural properties of the complexes. The EI mass spectra of the complexes show fragments corresponding to the evolved and intermediate species.

Keywords Thiourea derivative · Ni(II), Pd(II) and Pt(II) complexes · TG–DTA · Mass spectra

Introduction

Extensive studies on multidentate nitrogen–sulfur donors, especially those with NS or NNS sequence chelating agents, and their metal complexes. Such studies have led to new

compounds possess a wide range of biological applications [1–3]. As part of our efforts to explore new metal complexes of NS chelating agents that might exhibit beneficial therapeutic activity, we have reported the preparation and spectral characterization of *N*-allyl-*N'*-pyridin-2ylthiourea (AllPmTu) complexes of nickel(II), palladium(II), and platinum(II) [4] but no thermal studies have been reported. The mechanisms of thermal decomposition of some thioureas and their metal complexes have been reported [5, 6]. In this article, it is aimed at studying the mechanism of decomposition of these complexes in both solid and vapor states using TG, DTA, and electron impact mass spectral techniques, in order to support the mode of coordination of AllPmTu with Ni(II), Pd(II), and Pt(II) ions, and to assess the influence of the structural properties on their thermal behavior.

Experimental

Synthesis of complexes

The synthesis of the ligand, AllPm, and corresponding metal complexes are made by the procedures reported earlier [4]. Nickel(II) complexes were prepared from aqueous ethanolic solution of nickel(II)chloride and AllPmTu in mole ratios 1:1 and 1:2 (M:L). The complexes were characterized as a mixture of square planar/tetrahedral for $[Ni(AllPmTu)Cl_2(H_2O)]$ and as an octahedral for $[Ni(AllPmTu)_2Cl_2(H_2O)_2]$, in both complexes AllPmTu binds Ni^{II} as a monodentate ligand through a pyrimidine-N. Palladium(II) and platinum(II) were prepared by reacting aqueous solution of $[MCl_4]^{2-}$ with AllPmTu dissolved in EtOH in mole ratio 1:1, and $PtCl_2$ with AllPmTu in acetone in mole ratio 1:2. The complexes were characterized as a square planar for $[M(AllPmTu)Cl_2]$, $M = Pd^{II}$ or Pt^{II} and $[Pt(AllPmTu)_2]$ where AllPmTu binds

S. M. A. Katib (✉)
Department of Chemistry, Faculty of Applied Science,
Umm Al-Qura University, Makkah, P.O. Box 6831,
Kingdom of Saudi Arabia
e-mail: saudKatib@hotmail.com

M as a neutral bidentate through a pyrimidine-N and thiono-S, and binds Pt^{II} through a pyrimidine-N and thiolo-S atoms, respectively.

Instrumentation

The TG, DTG, and DTA curves were obtained using a Shimadzu-50 thermal analyzer. The measurements were performed in dynamic nitrogen atmosphere at a heating rate of $10\text{ }^{\circ}\text{C min}^{-1}$, using approximately 10 mg powdered samples contained in a platinum crucible. $\alpha\text{-Al}_2\text{O}_3$ is used as a reference material.

The electron impact mass spectra (EIMS) of the metal complexes were performed on a Finigan Mat 312 spectrometer operating at 70 eV electron energy. The ion source was set at $25\text{ }^{\circ}\text{C}$ and a direct insertion probe (DIP) was gradually heated from 50 to $300\text{ }^{\circ}\text{C}$. The electron amplifier was maintained at 1,500 V.

Results and discussion

Thermal analysis

The thermal behavior of AllPmTu metal complexes was studied by using TG and DTA techniques from ambient temperature up to $800\text{ }^{\circ}\text{C}$ in nitrogen flow, Figs. 1, 2, 3, 4, and 5. The stages of decomposition, temperature ranges, the temperature of the greatest rate of decomposition (DTG_{max}), the evolved products, as well as the found and calculated mass loss percentages of Ni(II), Pd(II), and Pt(II) complexes are given in Table 1.

[Ni(AllPmTu)Cl₂(H₂O)]

[Ni(AllPmTu)Cl₂(H₂O)] is thermally stable up to $150\text{ }^{\circ}\text{C}$ and decomposes beyond this temperature in a three stages as indicated in the TG curve. The mass loss at $292\text{ }^{\circ}\text{C}$

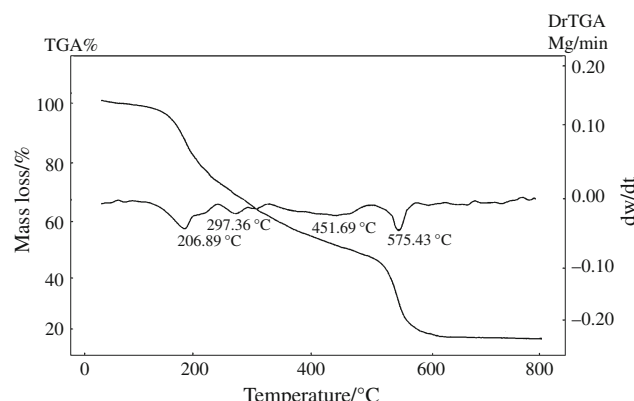


Fig. 1 TG and DTG curves of $[\text{Ni}(\text{AllPmTu})_2\text{Cl}_2(\text{H}_2\text{O})_2]$

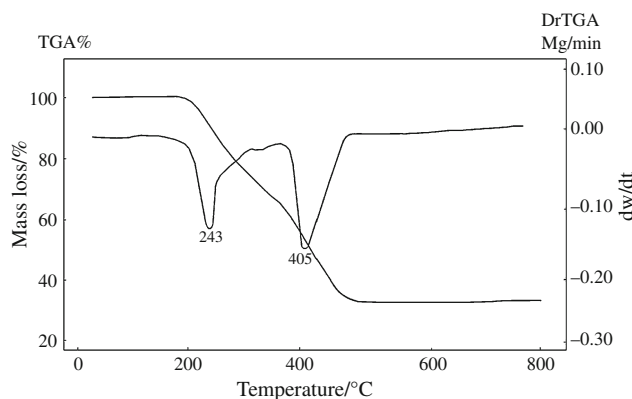


Fig. 2 TG and DTG curves of $[\text{Pd}(\text{AllPmTu})\text{Cl}_2]$

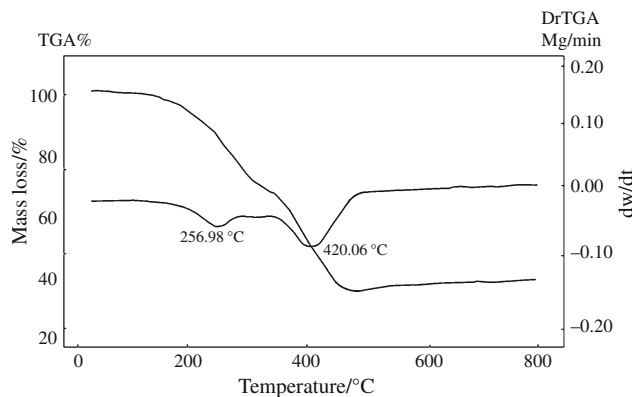


Fig. 3 TG and DTG curves of $[\text{Pt}(\text{AllPmTu})\text{Cl}_2]$

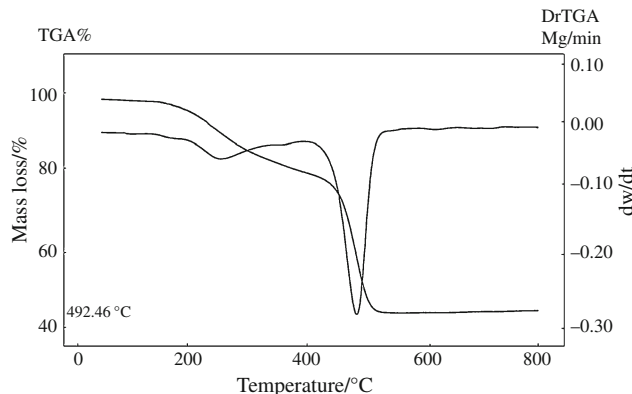


Fig. 4 TG and DTG curves of $[\text{Pt}(\text{AllPmTu})_2]$

corresponds to the formation of $[\text{Ni}(2\text{-amPm})(\text{H}_2\text{O})]$, where 2-amPm = 2-aminopyrimidine), as a result of elimination of allylisothiocyanate moiety. This is evident by the appearance in the EIMS a reasonable abundant species with m/z 99 corresponding to AllSCN^+ and a less abundant peaks corresponding to $[\text{Ni}(2\text{-amPm})\text{Cl}_2(\text{H}_2\text{O}) - 3]^+$ and $[\text{Ni}(\text{Pm})\text{Cl}_2(\text{H}_2\text{O})]^+$, as a result of the structural damages implicated in EI method due to both heating of the sample and production of ions with high internal energies. Beyond

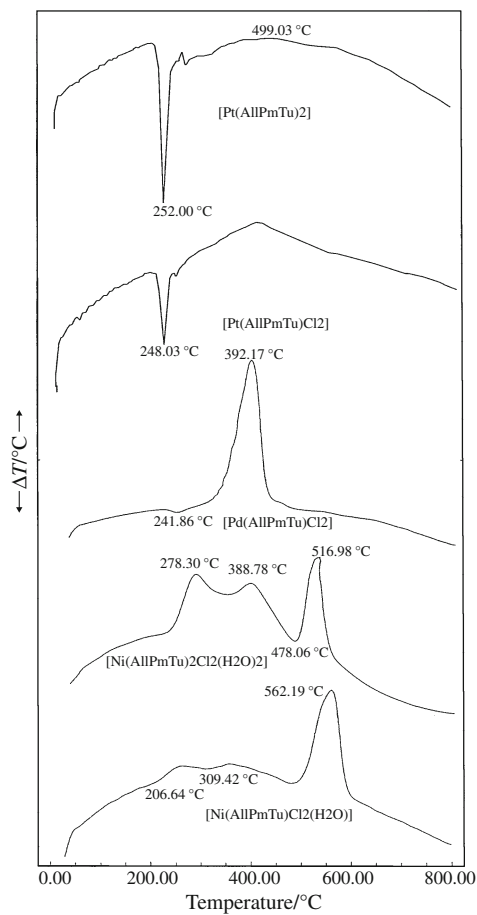


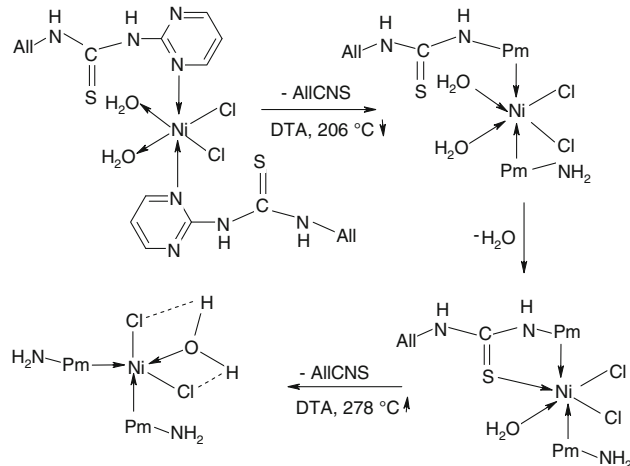
Fig. 5 DTA curves of AllPm Tu metal complexes

292 $^\circ\text{C}$, a second mass loss has been observed up to 472 $^\circ\text{C}$ corresponds to elimination of two HCl molecules and formation of $\text{NiO}(2\text{-amPm})$. The EIMS shows a peak at m/z 170 corresponds to $\text{NiO}(2\text{-amPm})^+$. Thereafter, the mass loss continues until a species attains a constant mass at 595 $^\circ\text{C}$, which corresponds to the formation of NiO. The DTA curve, Fig. 5, shows two endothermic peaks at 207 and 309 $^\circ\text{C}$ corresponding the decomposition of the complexes to $\text{NiO}(2\text{-amPm})$; one strong and broad exothermic peak at 562 $^\circ\text{C}$ corresponds to the decomposition of $\text{NiO}(2\text{-amPm})$ to NiO.

$[\text{Ni}(\text{AllPmTu})_2\text{Cl}_2(\text{H}_2\text{O})_2]$

The TG curve of $[\text{Ni}(\text{AlPmTu})_2\text{Cl}_2(\text{H}_2\text{O})_2]$, Fig. 1, is similar to that of $[\text{Ni}(\text{AlPmTu})\text{Cl}_2(\text{H}_2\text{O})]$ and indicates that the mass change begins at 173 $^\circ\text{C}$ and continues up to 598 $^\circ\text{C}$ in three stages. The initial mass loss in the temperature range 173–325 $^\circ\text{C}$ in the TG curve corresponds to the formation of $[\text{Ni}(2\text{-amPm})_2\text{Cl}_2(\text{H}_2\text{O})]$ with three DTG_{max} values at 207, 242, and 297 $^\circ\text{C}$. The appearance of several DTG peaks for this step indicates that the greatest rates of decomposition of the three species, one H_2O plus

two allylisothiocyanate, occurs at different temperatures and that the mechanism of decomposition is not straightforward and may be speculated as:



The DTA curve, Fig. 5, shows one endothermic peak at 206 $^\circ\text{C}$ corresponding to the elimination of one allylisothiocyanate moiety and no peak for elimination of H_2O molecule, suggesting that the heat consumed in elimination of H_2O is nearly cancelled out by the heat evolved on bond formation between thioketo sulfur and nickel(II). The second mass loss occurs in the temperature range 325–481 $^\circ\text{C}$ on the TG curve which corresponds to elimination of 2 HCl molecules and formation of $(2\text{-APm})_2\text{NiO}$. Beyond 481 $^\circ\text{C}$, a continuous mass loss is observed up to 598 $^\circ\text{C}$ which corresponds to the decomposition of $(2\text{-Pm})_2\text{NiO}$ to NiO. The DTA profile, Fig. 5, also shows two exothermic peaks at 389 and 571 $^\circ\text{C}$ corresponding to the decomposition of the intermediate species with elimination of 2 HCl and 2(2-APm) molecules, respectively, and formation.

$[\text{Pd}(\text{AllPmTu})\text{Cl}_2]$

The TG curve of $[\text{Pd}(\text{AllPmTu})\text{Cl}_2]$, Fig. 2, shows an initial mass loss in the temperature range 221–265 $^\circ\text{C}$ with a DTG_{max} at 257 $^\circ\text{C}$ corresponding to the elimination of allylimine moiety. This is followed by another mass loss in the temperature range 265–452 $^\circ\text{C}$ with a DTG_{max} at 405 $^\circ\text{C}$ due to decomposition of 2-cyanopyrimidine radical plus 2HCl molecules and formation of PdS. The DTA profile, Fig. 5, shows one weak endothermic peak at 242 $^\circ\text{C}$ corresponds to the elimination of allylimine molecule and formation of $[\text{Pd}(\text{PmNHCHS})]$ and one relatively broad strong exothermic peak at 420 $^\circ\text{C}$ corresponding to the decomposition of the last intermediate to PdS and dimerization (of) PmNC radical.

Table 1 Thermoanalytical results of metal complexes of *N*-allyl-*N'*-pyrimidin-2-ylthiourea

Complex	Stage	Temperature range/°C	DTG _{max} /°C	Mass loss/%		Evolved moiety	DTA peak/°C
				Found	Theor.		
[Ni(AllPmTu)Cl ₂ (H ₂ O)] (341.7)	I	150–292	243			C ₄ H ₅ NS	252 (exo)
	II	292–472	427	29.23	29.03	2HCl	359 (exo)
	III	472–595	529	21.40	21.41	2-APm	562 (exo)
	Residue	>595	–	27.55	27.85	NiO	–
				21.97	21.86		
[Ni(AllPmTu) ₂ Cl ₂ (H ₂ O) ₂] (553.7)	I	173–325	207, 297			H ₂ O + 2C ₄ H ₅ NS 2HCl	206(endo), 278(exo)
	II	325–481	452	38.70	38.06	2(2-APm)	389 (exo)
	III	481–598	575	13.10	13.18	NiO	571 (exo)
	Residue	>598	–	34.25	34.31		–
				13.95	13.49		
[Pd(AllPmTu)Cl ₂] (371)	I	221–265	243			C ₃ H ₅ N ^a 2HCl + PmNC PdS	242(endo)
	II	265–452	405	14.6	14.8		392(exo)
	Residue	>452	–	48.10	47.97		–
				37.30	37.19		
[Pt(AllPmTu)Cl ₂] (460)	I	195–265	257			C ₃ H ₅ N 2HCl + PmNC PtS	243(endo)
	II	265–481	420	12.05	11.95		441(exo)
	Residue	>481	–	38.40	38.69		–
				49.55	49.34		
[Pt(AllPmTu) ₂] (583)	I	195–385	269			2 C ₃ H ₅ NH ₂ PmNC+ PmNCS	252(endo)
	II	385–535	492	20.03	19.55		499(exo)
	Residue	>535	–	41.87	41.50	PtS	
				38.10	38.93		

^a HN=CH–CH=CH₂; Pm: pyrimidine; 2-APm: 2-aminopyrimidine

[Pt(AllPmTu)Cl₂]

The TG curve of [Pt(AllPmTu)Cl₂], Fig. 3, shows a two steps of decomposition similar to that of [Pd(AllPmTu)Cl₂]. The initial mass loss is in the temperature range 195–269 °C with a DTG_{max} at 257 °C, corresponding to decomposition of allylamine moiety. The second step of decomposition shows a mass loss, in the temperature range 269–481 °C with a DTG_{max} at 420 °C, which is consistent with elimination of PmNC radical and Cl₂ with the formation of PtS as the end product at 481 °C and up to 800 °C. The DTA curve, Fig. 5, shows an endothermic peak at 243 °C corresponding to elimination of allylimine moiety and a broad strong exothermic one at 441 °C due to thermal decomposition of the remaining complex to PtS.

[Pt(AllPmTu)₂]

The TG curve of [Pt(AlPmTu)₂], Fig. 4, shows two steps of decomposition. The first step is in 195–385 °C range with a DTG_{max} at 269 °C, which corresponds to elimination of two allylamine molecules. The other decomposition step occurs in the temperature range 385–535 °C with a DTG_{max} at 492 °C and corresponds to elimination of

PmNC radical plus PmSCN molecule [5] with the formation of PtS. The DTA profile, Fig. 5, shows an endothermic peak at 252 °C and a broad strong exothermic peak at 499 °C which correspond to decomposition of 2-cyano-pyrimidine radical plus a PmNC radical plus pyrimidin-2-ylisothiocyanate molecule with the formation of PtS.

In order to asses the influences of the mode of bonding of the ligand to the metal ions and the structural properties of the complexes on their thermal behavior, the order, *n*, and the heat of activation *E*[#] of the various decomposition stages were determined from the TG and DTG thermograms using the Coats–Redfern equations [7, 8] in the following form:

$$\ln \left[\frac{1 - (1 - \alpha)^{1-n}}{(1-n)T^2} \right] = \frac{M}{T} + B \quad \text{for } n \neq 1, \quad (1)$$

$$\ln \left[\frac{-\ln(1 - \alpha)}{T^2} \right] = \frac{M}{T} + B \quad \text{for } n = 1 \quad (2)$$

where *M* = *E*[#]/*R* and *B* = ln*A*R/Φ*E*[#]; *E*[#], *R*, *A*, and Φ are the heat of activation, universal gas constant, pre-exponential factor, and heating rate, respectively. The correlation coefficient, *r*, was computed using the least squares methods for different values of *n*, by plotting the left-hand

Table 2 Temperature of decomposition and activation parameters of AllPmTu metal complexes

Complex	Step	T/K	r	A/s ⁻¹	E [#] /kJmol ⁻¹	ΔH [#] /kJmol ⁻¹	ΔS [#] /kJmol ⁻¹	ΔG [#] /kJmol ⁻¹
[Ni(AllPmTu)Cl ₂ (H ₂ O)]	1st	516	0.997371	4.21 × 10 ¹¹	63.55	59.26	-0.027	73.16
	2nd	700	0.996741	7.88 × 10 ⁹	61.69	55.87	-0.063	99.66
	3rd	802	0.995710	2.58 × 10 ¹²	210.86	204.18	-0.016	217.02
[Ni(AllPmTu) ₂ Cl ₂ (H ₂ O) ₂]	1st	570	0.998951	8.83 × 10 ⁹	46.58	41.84	-0.091	93.14
	2nd	725	0.997929	1.46 × 10 ¹¹	76.40	70.37	-0.063	116.05
	3rd	848	0.988911	2.69 × 10 ¹²	206.07	199.02	-0.016	212.28
[Pd(AllPmTu)Cl ₂]	1st	516	0.981165	3.08 × 10 ¹²	71.44	67.15	-0.017	75.92
	2nd	678	0.953508	3.50 × 10 ⁷	42.68	37.04	-0.107	109.81
[Pt(AllPmTu)Cl ₂]	1st	516	0.990819	5.42 × 10 ⁹	46.31	42.02	-0.064	74.59
	2nd	693	0.980238	7.51 × 10 ⁸	48.11	42.35	-0.082	99.18
[Pt(AllPmTu) ₂]	1st	542	0.998395	1.00 × 10 ¹¹	84.55	80.04	-0.039	101.18
	2nd	765	0.903803	6.56 × 10 ⁸	92.38	86.02	-0.084	150.24

side of the Eqs. 1 and 2 versus $1,000/T$. The n value which gave the best fit ($r \cong 1$) was chosen as the order parameter for the decomposition stage of interest. From the intercept and linear slope of such stage, the A and $E^{\#}$ values were determined. The other kinetic parameters, $\Delta H^{\#}$, $\Delta S^{\#}$ and $\Delta G^{\#}$ were computed using the relationships: $\Delta H^{\#} = E^{\#} - RT$, $\Delta S^{\#} = R[\ln(Ah/kT) - 1]$ and $\Delta G^{\#} = \Delta H^{\#} - T\Delta S^{\#}$, where k is the Boltzmann's constant and h is the Planck's constant. The kinetic parameters are collected in Table 2. The following remarks can be pointed out:

- (i) The negative values of the $\Delta S^{\#}$ indicate a more ordered activated state than the reactants [9].
- (ii) The values of the $\Delta G^{\#}$ increases markedly for the subsequent decomposition stages of a given complex, though there is no obvious trends in the values of either $E^{\#}$ or $\Delta H^{\#}$. This is due to increasing the values of $T\Delta S^{\#}$ from one step to another which override the values of $\Delta H^{\#}$. Increasing the values of $\Delta G^{\#}$ for the subsequent steps of a given complex reflects that the rate of removal of the subsequent species will be lower than that of the precedent species [10, 11]. This may be attributed to the structural rigidity of the remaining complex after the expulsion of one or more species, as compared with the precedent complex.
- (iii) The values of $\Delta G^{\#}$ of the first step of decomposition of the two structurally analogous, square-planar d⁸ complexes, [M(AllPmTu)Cl₂], M = Pd^{II} or Pt^{II}, are nearly equal, since this step is metal independent, but $\Delta G^{\#}$ values of the second step of the two complexes are different ($\Delta G_{\text{Pd}}^{\#} > \Delta G_{\text{Pt}}^{\#}$), reflecting that the rate of decomposition of this step involves the coordination core and reveals a relatively higher thermal stability of Pt(II) complex as compared to Pd(II) one.
- (iv) The $\Delta G^{\#}$ value for the first step, which involves the coordination core, of the four-coordinate nickel(II)

complex, [Ni(AllPmTu)Cl₂(H₂O)], is lower than that the octahedral one, [Ni(AllPmTu)₂Cl₂(H₂O)₂]. This may be attributed to the larger values of CFSE of octahedral than that of the tetrahedral and square-planar nickel(II) complexes. The difference in $\Delta G^{\#}$ values of the subsequent steps becomes smaller, since the structure of the intermediate complexes becomes similar.

- (v) The $\Delta G^{\#}$ values of [Pt(AllPmTu)₂] are higher than that of [M(AllPmTu)Cl₂], reflecting a higher thermal stability of ML₂ in terms of chelate effect.
- (vi) The reaction orders for all decomposition stages of all complexes are found to be nearly equal unity. It was emphasized that the order of a solid-state decomposition reaction has no intrinsic meaning, but is rather a mathematical smoothing parameter [12].

References

1. del Campo R, Criado JJ, García E, Hermosa MR, Sánchez AJ, Manzano JL, Monte E, Fernández ER, Sanz F. Thiourea derivatives and their nickel(II) and platinum(II) complexes: antifungal activity. *J Inorg Biochem* 2002;89:74–82.
2. Padhye SB, Kauffman GBT. Transition metal complexes of semicarbazones and thiosemicarbazones. *Coord Chem Rev*. 1985;63:127–60.
3. Colebunder RL, Ryder GF, Nzialambi N. HIV infection in patients with tuberculosis in Kinshasa, Zaire. *Am Rev Respir Dis*. 1989; 139:1082–5.
4. Kandil SS, Katib SMA, Yarkandi NHM. Nickel(II), palladium(II) and platinum(II) complexes. *Transition Met Chem*. 2007;32: 791–8.
5. Lizarraga E, Zabaleta C, Palop JA. Mechanism of thermal decomposition of thiourea derivatives. *J Therm Anal Calorim*. 2008;93:887–98.
6. Özpozan N, Arslan H, Özpozan T, Özdes N, Külcü N. Thermal studies of Ni(II), Pt(II) and Ru(III) complexes of N, N-dihexyl-N'-benzoylthiourea. *Thermochim Acta*. 2000;343:127–33.

7. Coats AW, Redfern JP. Kinetic parameters from thermogravimetric data. *Nature*. 1964;201:68–9.
8. Avsar G, Altinel H, Yilmaz MK, Guzel B. Synthesis, characterization, and thermal decomposition of fluorinated salicylaldehyde Schiff base derivatives (Salen) and their complexes with copper(II). *J Therm Anal Calorim*. 2010;101:199–203.
9. Forst AA, Pearson RG. Kinetics and mechanisms. New York: Wiley; 1961.
10. Maravalli and Goudar TR PB, Goudar TR. Thermal and spectral studies of 3-N-methyl-morpholino-4-amino-5-mercaptop-1,2,4-triazole and 3-N-methyl-piperidino-4-amino-5-mercaptop-1,2,4-triazole complexes of cobalt(II), nickel(II) and copper(II). *Thermochim Acta*. 1999;325:95–105.
11. Yusuff KKM, Sreekala R. Thermal and spectral studies of 1-benzyl-2-phenylbenzimidazole complexes of cobalt(II). *Thermochim Acta*. 1990;159:357–68.
12. Brown DB, Walton EG, Dits JA. Thermal reactions of the mixed valence iron flourides, $\text{Fe}_2\text{F}_6 \cdot n\text{H}_2\text{O}$. *J Chem Soc Dalton Trans*. 1980;845–50.